Phase coherence in the hysteretic magnetic behavior of parallel Josephson-junction arrays

J. H. Miller, Jr.
Department of Physics and Texas Center for Superconductivity, University of Houston, 4800 Calhoun Road, Houston, Texas 77204-5932

G. H. Gunaratne
Department of Physics, University of Houston, 4800 Calhoun Road, Houston, Texas 77204-5506

Z. Zou
Department of Physics and Texas Center for Superconductivity, University of Houston, 4800 Calhoun Road, Houston, Texas 77204-5932

M. F. Davis, H. R. Rampersad, and J. C. Wolfe
Department of Electrical Engineering and Texas Center for Superconductivity, University of Houston, 4800 Calhoun Road, Houston, Texas 77204-5932
(Received 21 January 1994)

We report on the hysteretic field-dependent critical currents of large inductance arrays with up to ten $YBa_2Cu_3O_7$ grain-boundary junctions in parallel. A peak in the critical current, roughly equal to its initial zero-field value, is observed after each reversal of the field sweep. This behavior indicates that the junction phases become equal modulo 2π (self-organized phase coherence) as the system relaxes away from the critical state. The primary features can be modeled using a Frenkel-Kontorova model generalized to include global interactions due to mutual inductance.

Most work reported to date on Josephson-junction (JJ) arrays[1] has concentrated on arrays in which the inductance can be neglected. The large inductance limit can lead to interesting metastable phenomena which have not been extensively studied thus far. The "magnetization" vs field (M-H) curve of a JJ array with finite inductance is predicted[2] to exhibit a hysteresis loop nearly identical to that of the Bean critical state model.[3] A one-dimensional (1D) array, consisting of many JJ's in parallel, can be represented by the Frenkel-Kontorova (FK) model[4] of spring-coupled balls in a washboard potential, provided only self-inductance terms are included. In the "critical state" of such an array, each junction carries its critical current, and the difference between the amount of flux trapped in adjacent loops is roughly equal to the product of the loop inductance and the critical current.[5]

We recently measured the hysteretic field-dependent critical currents of 1D parallel JJ arrays with large inductance. We observed a pronounced maximum in the critical current after each reversal of the field sweep. This behavior suggests that the phases across the junctions spontaneously become coherent as the system relaxes away from its critical state. We modeled the observed behavior by generalizing the FK model to include global interactions due to mutual inductance. Rather surprisingly, we found the globally coupled FK model to exhibit several essential aspects of the experimental behavior not shown by identical simulations using the conventional FK model.

The arrays consisted of up to ten Josephson junctions in parallel, fabricated by patterning 1400-Å-thick $YBa_2Cu_3O_7$ films deposited onto $SrTiO_3$ bicrystal substrates with 24° misorientation angles.[6] The width of each junction was 5 μm and the dimensions of each loop in the array were 10 μm$\times$50 μm. The films were laser deposited using a KrF pulsed excimer laser and were patterned using photolithography and ion milling. Resistively shunted junction (RSJ)-like behavior was observed in the current-voltage (I-V) characteristics.[7] The self-inductance of each loop L was estimated to be $\sim$40 pH, and the self-inductance parameter $\beta_L = 2LI_0/\phi_0$ ranged from less than 10 just below the critical temperature to over 100 at 4 K, due to the temperature dependence of the critical current. Here L is the self-inductance of each loop, I_0 is the critical current, assumed to be the same for each junction, and $\phi_0 = h/2e$ is the flux quantum. The ability to substantially change device parameters simply by changing the temperature is an important advantage of using high-T_c grain-boundary junctions for this study, in addition to their being self shunting and easy to fabricate. A dc current applied to a Helmholtz coil was used to control the magnetic field. The measurements were conducted in a radio frequency (rf) shielded enclosure and the cryostat was magnetically shielded inside a double μ-metal can. A feedback circuit was utilized for most of the critical current vs field (I_c-H) measurements. The circuit was designed to adjust the total current in order to maintain a fixed voltage of $\sim$1 μV across the junction array. Fraunhöfer-like I_c-H characteristics with no magnetic hysteresis, indicative of Josephson-type behavior, were observed in single bicrystal junctions fabricated on the same substrate.

Figure 1 shows the magnetic-field dependence of the

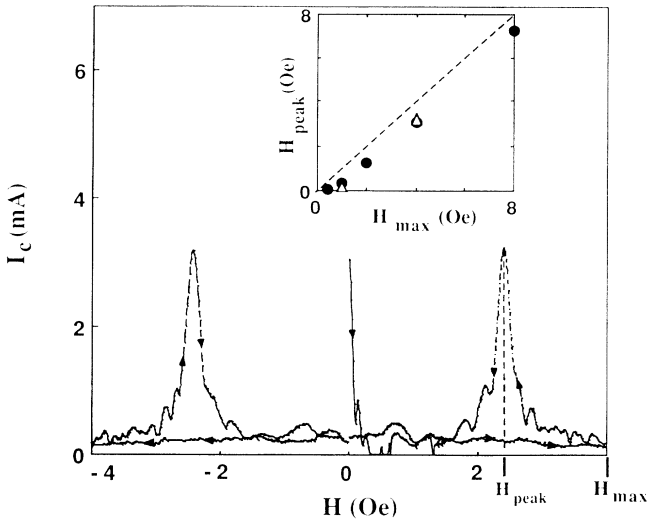

FIG. 1. Critical current vs field for a ten-JJ array at 77 K ($\beta_L \sim 13$). The field begins at zero and is slowly increased to its maximum positive value. The sweep is then reversed and the field is swept to its maximum negative value. Finally, the field is slowly swept back to zero. Inset: Plot of H_{peak} vs H_{max} for a six-JJ array (circles) and a ten-JJ array (open triangles) at 77 K. The dashed line corresponds to setting $H_{peak}=H_{max}$.

critical current for a ten-junction interferometer. The array is cooled in zero field to the operating temperature. As the field is increased, the critical current decreases to a small residual value, showing small periodic oscillations. On reversing the field sweep, a pronounced "satellite" peak is observed. Further reversals of the sweep directions yield only the satellite peaks, as seen in Fig. 1, while the central maximum originally observed in zero field becomes suppressed until the sample is warmed up above T_c and cooled down again in zero field. This behavior is somewhat reminiscent of the hysteresis in the field-dependent critical currents of granular superconducting (e.g., Nb) microbridges.[8] The magnetic fields were sufficiently low that the observed hysteretic behavior was primarily the result of flux (up to $\sim N\beta_L/2$ flux quanta per loop) being trapped in the rather large inductance loops instead of at pinning sites in the film.

After the array is initially cooled in zero field, the critical current is simply given by $\sum I_{ci}\sin\theta_i=\sum I_{ci}$, where I_{ci} is the critical current of the ith junction and the junction phases $\theta_i=\pi/2$ are all identical. In general, the phase across each junction must be equal to $\pi/2+2\pi m$, where m is an integer, in order for the total current to be equal to its maximum value. When a magnetic field is applied, the phases are related by $\theta_i=\theta_{i-1}+2\pi\phi_i/\phi_0$, where ϕ_i is the flux through the ith loop, which includes contributions from the applied field and the circulating currents. The fact that the critical current at the satellite peaks is about as large as its initial zero-field value implies that the phases have adjusted themselves such that $\theta_i=\theta_{i-1}+2\pi n_i$, where n_i is an integer, and an integral number of flux quanta are present in each loop. We call this phenomenon *self-organized phase coherence.* A likely explanation, which is borne out by our detailed model calculations described below, is that the phases simultaneously relax to minima in the periodic potential as the system relaxes away from the critical state.

The magnetic field H_{peak} corresponding to the position of the dominant satellite peak depends on the sweep range, or maximum applied field H_{max}, as shown in the inset to Fig. 1. However, the difference $\Delta H^*=|H_{max}-H_{peak}|$ between the maximum applied field and the position of the satellite peak is roughly independent of H_{max} at a fixed temperature, provided that $|H_{max}|>2\Delta H^*$. The value of ΔH^* thus appears to be related to the field required for the system to reach the critical state. If the temperature is reduced (thereby increasing the maximum critical current and value of β_L) the satellite peaks become broader and ΔH^* increases, as shown in Fig. 2.

We suggest that the hysteretic behavior of the critical current peak results from the effects of long-range inductance of the JJ array. This assumption leads us to a simple generalization of the Frenkel-Kontorova model to include global interactions, as we show below. Let us consider first an infinite "ladder" of JJ's arranged in parallel, as illustrated in Fig. 3. ϕ_i is the flux trapped inside the ith loop, while θ_i is the time-dependent phase across the ith JJ. We express the current as a sum of circulating current loops, I_i being the circulating current in the ith loop. The current flowing through the ith junction is simply the difference between the adjacent circulating currents (I_i-I_{i+1}). In the RSJ model, neglecting the junction capacitance and taking the junction critical currents $I_{ci}=I_0$ to be identical, the Josephson relations for the ith junction give

$$I_i-I_{i+1}=I_0\sin\theta_i+\frac{\phi_0}{2\pi R}\frac{d\theta_i}{dt}\ , \tag{1}$$

where R is the shunt resistance of each junction. The net flux ϕ_i in the ith loop is related to the phases across the adjacent junctions by

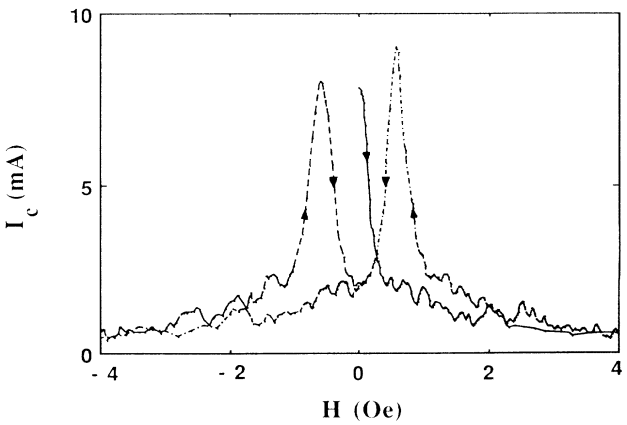

FIG. 2. Critical current vs field for the ten-JJ array at 40 K. Note the broadening of the peaks due to the increased critical current ($\beta_L \sim 32$).

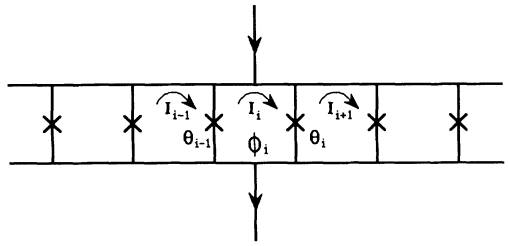

FIG. 3. Infinite ladder of JJ's in parallel.

$$\phi_i=\frac{\phi_0}{2\pi}(\theta_i-\theta_{i-1}) . \tag{2}$$

ϕ_i can also be written as the sum of the externally applied flux per loop $\phi_{\rm ext}$ and the flux inductively coupled into the ith loop from all of the individual current loops in the array, i.e.,

$$\phi_i=\phi_{\rm ext}-\sum_j L_{ij}I_j . \tag{3}$$

Here L_{ij} measures the flux in loop i due to the current I_j circulating in the jth loop.

Most analyses include only the self-inductances (L_{ii}) and ignore the mutual inductances L_{ij} ($i\neq j$). Then the phase differences $\{\theta_i\}$ satisfy the FK model, whose mechanical analog is an array of identical masses on a sinusoidal potential, in which the nearest neighbors are coupled by springs. In the high-inductance limit considered here, the assumption $L_{ij}=0 (i\neq j)$ is unacceptable, and we study the effects of relaxing this assumption. The contributions to the flux coupled into loop i by the circulating currents I_j ($j\neq i$) have the opposite sign vs that of the self-induced flux, since points in the ith loop lie outside of loop j. Hence $L_{ii}>0$ while $L_{ij}<0$ for $i\neq j$. Further, L_{ij} is assumed to decay rapidly with increasing $|i-j|$, since mutual inductive couplings tend to decay rapidly with increasing distance between the loops when the loops all lie in a plane and do not overlap.[9] Under these conditions Eq. (3) can be inverted to give

$$I_i=\sum_j M_{ij}(\phi_{\rm ext}-\phi_j)=\left[\sum_j M_{ij}\right]\phi_{\rm ext}-\sum_j M_{ij}\phi_j , \tag{4}$$

where $\{M_{ij}\}$ is a symmetric matrix with positive elements that decays rapidly as one moves away from the diagonal. For the infinite array of identical JJ's, M_{ij} depends only on $|i-j|$. Hence

$$\begin{aligned} I_i-I_{i+1}&=-\sum_j M_{ij}\phi_j+\sum_j M_{i+1j}\phi_j \\ &=I_0\sum_n \lambda_n(\theta_{i+n}-2\theta_n+\theta_{i-n}) , \end{aligned} \tag{5}$$

where $\lambda_n I_0=(\phi_0/2\pi)[m_{n-1}-2m_n+m_{n+1}]$, with $m_{n'}=M_{i,i+n'}$. Substitution into Eq. (1) gives

$$\frac{d\theta_i}{dt}=\omega_0\left[-\sin\theta_i+\sum_n \lambda_n(\theta_{i+n}-2\theta_i+\theta_{i-n})\right] , \tag{6}$$

where $\omega_0=2\pi I_0 R/\phi_0$.

This is the equation of motion for an infinite set of globally coupled masses moving in a sinusoidal potential in the highly viscous limit. We are thus motivated to introduce a corresponding model for a finite array of JJ's:

$$\frac{d\theta_i}{d\tau}=-\sin\theta_i+\sum_n \lambda_n(\theta_{i+n}-\theta_i-2\pi nh) , \tag{7}$$

where $\tau=\omega_0 t$ is a dimensionless time variable, the summation being over all JJ phases. The mechanical analog of this generalized FK model is a finite set of identical particles sitting in a sinusoidal potential and moving in the high viscosity limit. The particles are globally coupled by springs, the spring constant of that joining the ith and jth particles being $\lambda_{|i-j|}$, while its length is $|i-j|\cdot h$, where $h=\phi_{\rm ext}/\phi_0$ is proportional to the applied magnetic field ($\theta_i/2\pi$ = position of the ith particle). In the FK model, $\lambda_{\pm 1}=1/\pi\beta_L$, and $\lambda_n=0$ when $n\neq\pm 1$. We do not expect this simple model to exhibit all of the complex properties of the JJ array. Rather, what we are attempting here is to qualitatively understand the large peaks in critical current.

We start the system with $\phi_{\rm ext}=0$ (i.e., $h=0$), and all particles in the bottom of a single potential well. We then increase h in steps of Δh, each time evolving the system via Eq. (7) until it reaches equilibrium. For each value of h we compute the equilibrium phases θ_i^0, the normalized flux of each loop ϕ_i/ϕ_0, and the magnetization $m\equiv\langle\phi_i/\phi_0-h\rangle_{\rm ave}$ in order to generate an m vs h hysteresis loop. The total current $\sum\sin\theta_i^0$ is equal to zero when the system is in equilibrium. Figures 4(a) and 4(c) show m-h hysteresis loops for a ten-JJ array using parameters roughly corresponding to the experimental data of Figs. 1 and 2, respectively.[10] The hysteresis loops are similar to those of the critical state model. Many flux quanta become trapped in each loop of the array due to the circulating currents and finite inductances, whereas flux vortices trapped in the body of the superconductor play a minimal role here.

Once equilibrium is established for a given field, as the bias current is increased from zero, the flux ϕ_i in each loop will remain unchanged, provided the system does not undergo a transition into a new metastable state. Such transitions into different metastable configurations have been observed by us experimentally, in the form of sudden "jumps" in critical current, but such jumps tend to occur rather infrequently during a period of many minutes, or even hours. We therefore define the critical current to be the maximum possible bias current for a given metastable configuration. The effect of the bias current is to add a transport current $I_{ti}=\sin\theta_i-\sin\theta_i^0$ to the right-hand side of Eq. (7),[11] where θ_i represents the junction phase in the presence of the bias current. Note that the same basic metastable configuration is maintained,[12] and that the modified form of Eq. (7) continues to be satisfied, provided we take $\theta_i=\theta_i^0+\delta\theta$, where $\delta\theta$ is

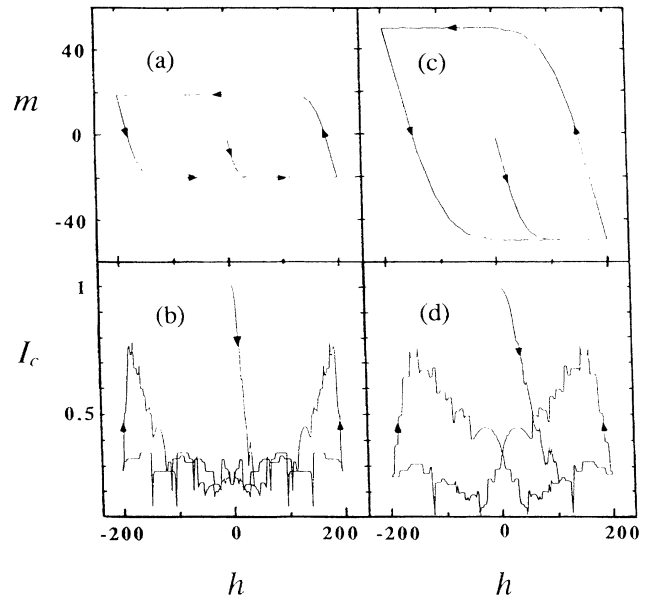

FIG. 4. (a) and (c): Magnetization vs field (m-h) in units of Φ_0 per loop for a ten-JJ array, using parameters roughly corresponding to the data of Figs. 1 and 2, respectively. (b) and (d): Normalized critical current vs field using the same parameters as those used for (a) and (c), respectively.

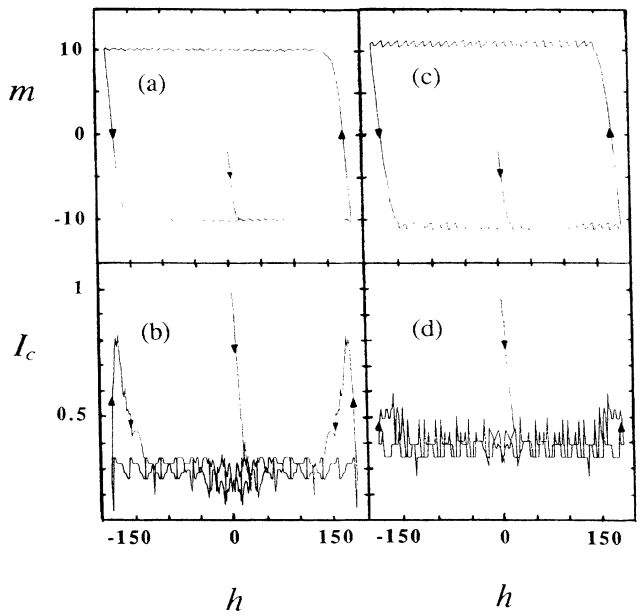

FIG. 5. Magnetization vs field (m-h) for a ten-JJ array using (a) a globally coupled FK model with $\lambda_n = 0.05/n^2$, and (c) a locally coupled FK model with $\lambda_{\pm 1} = 0.25$ and $\lambda_n = 0$ for $|n| \geq 2$. The parameters were chosen to yield similar m-h curves. (b) (globally coupled FK model) and (d) (locally coupled FK model): normalized critical current vs field using the same parameters as those used for (a) and (c), respectively.

the same for all of the junctions. The critical current is then given by the maximum total bias current, $\sum I_{ti} = \sum \sin\theta_i - \sum \sin\theta_i^0 = \sum \sin\theta_i$.

These quasistatic calculations are not completely compatible with the experimental measurements, in which a feedback circuit maintained a finite voltage of about 1 μV across the array. However, we observed essentially the same behavior by incrementing the magnetic field while zero-bias current was applied and then applying short rectangular current pulses in order to determine the critical current for each value of magnetic field. The plots of I_c vs H thus obtained looked essentially the same as those of Figs. 1 and 2. Unfortunately, data obtained using the pulsed technique had to be taken by hand, and, therefore, the plots lacked the wealth of detail obtained by automated data acquisition (Figs. 1 and 2). Nevertheless, the fact that essentially the same results were obtained by the two methods, indicates that our experimental measurements yielded at least a reasonable approximation of the true, quasistatic critical current.

Figures 4(b) and 4(d) show theoretical plots of normalized critical current vs field corresponding to the m-h hysteresis loops in Figs. 4(a) and 4(c), respectively. When the field is initially increased from zero, the critical current reduces to a minimum value as the system reaches the critical state. The experimentally observed satellite peaks in the critical current, and the observed broadening with increasing β_L, are reproduced in these theoretical plots. However, whereas the experimentally observed satellite peaks have nearly symmetric profiles, which are substantially offset from the maximum applied field, the theoretical peaks are quite asymmetric and they do not quite attain the maximum (zero-field) critical current. Nevertheless, the agreement is substantially better than our attempts to model the observed behavior using the locally coupled FK model, and suggests the inclusion of global coupling in finite-inductance calculations.

Figures 5(a)–5(d) show a direct comparison of theoretical m-h and I_c-H plots, obtained using globally-coupled and locally-coupled FK models. Note that the locally

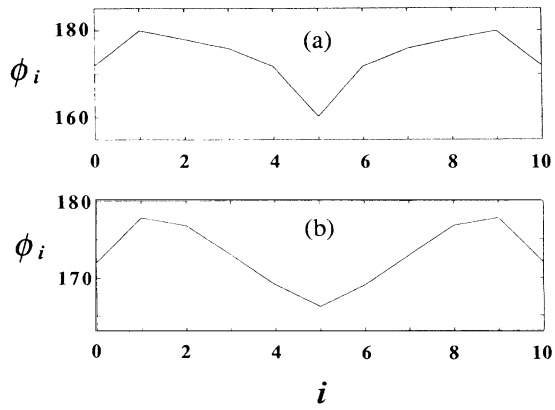

FIG. 6. Number of trapped flux quanta per loop ϕ_i/ϕ_0 vs loop number i (1–9) for (a) the globally coupled FK model with $\lambda_n = 0.05/n^2$, and (b) the locally coupled FK model with $\lambda_{\pm 1} = 0.25$. Both plots correspond to the case where $m = 0$ on the right-hand sides of the m-h hysteresis curves in Fig. 5. The externally applied flux ϕ_{ext}/ϕ_0 is plotted at the points $i = 0$ and $i = 10$.

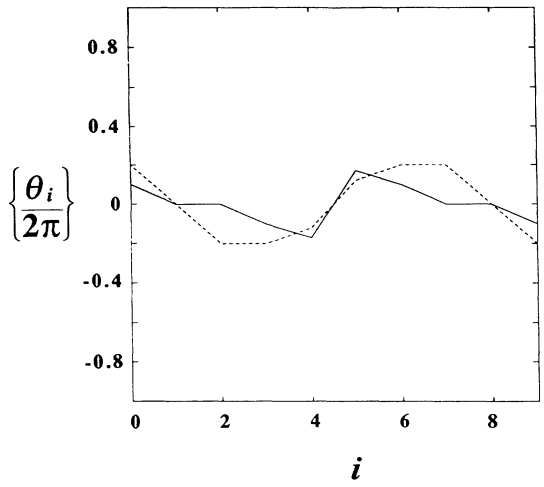

FIG. 7. Normalized junction phase modulo 2π, $\{\theta_i/2\pi\}$, vs junction number i for (solid line) the globally coupled FK model with $\lambda_n=0.05/n^2$, and (dotted line) the locally coupled FK model with $\lambda_{\pm 1}=0.25$. Both plots correspond to zero magnetization, as in Fig. 6.

coupled FK model predicts that the critical current peaks are substantially less pronounced than those predicted by the globally coupled FK model, despite the fact that the parameters were chosen to yield similar m-h curves. We have found that the globally coupled FK model always predicts much larger critical current peaks than the locally coupled FK model, regardless of the specific choice of coupling parameters. Figures 6(a) and 6(b) show profiles of flux per loop ϕ_i/ϕ_0 vs loop number i for the globally coupled and locally coupled FK models, respectively, corresponding to zero magnetization ($m=0$) at the right-hand sides of the m-h curves in Fig. 5. These plots are similar to plots of flux density vs position in the Bean critical state model, and show that having zero net magnetization is not a sufficient condition for the total critical current to be large, since substantial flux is still trapped in each loop.

The reason for the different behaviors of the global vs local models can be seen by examining the junction phases when the magnetization is zero. Figure 7 shows plots of the normalized junction phases modulo 2π, $\{\theta_i/2\pi\}$, in the absence of a bias current, for $m=0$, as in Fig. 6. Careful examination of Fig. 7 reveals that more phases have relaxed close to the minima in the periodic potential for the globally coupled FK model than for the locally coupled model. This suggests that, as the system moves away from the critical state and the "springs" relax, the phases in the globally coupled model simultaneously relax close to the nearest minima in the sinusoidal potential, resulting in phase coherence modulo 2π. The opposite critical state is attained as the field continues to sweep in the opposite direction. The phases lose their coherence as they move away from the metastable minima, and the total critical current again becomes small. We have found that the qualitative predictions of the globally coupled FK model do not depend on the detailed n dependence of the coupling constants λ_n provided they decrease with n.

In conclusion, we have observed evidence for self-organized phase coherence in the magnetic behavior of parallel JJ arrays, and have interpreted this phenomenon using a generalized FK model which includes global interactions. We believe that the importance of global coupling extends to the behavior of other systems, such as charge-density waves and flux lattices in type-II superconductors.

We would like to express our appreciation to S. C. Bechtold, N. Q. Fan, N. Fogo, and Y. Wang for their assistance. This research was supported by the state of Texas through the Texas Center for Superconductivity, the Advanced Technology Program, the Energy Laboratory, and the Institute for Space Systems Operations, and by the Robert A. Welch Foundation and (GHG) the Office of Naval Research.

[1]See, for example, S. P. Benz, M. S. Rzchowski, M. Tinkham, and C. J. Lobb, Phys. Rev. Lett. **64**, 693 (1990); D. C. Harris, S. T. Herbert, D. Stroud, and J. C. Garland, *ibid.* **67**, 3606 (1991).

[2]A. Majhofer, T. Wolf, and W. Dietrich, Phys. Rev. B **44**, 9634 (1991).

[3]C. P. Bean, Phys. Rev. Lett. **8**, 250 (1962).

[4]Y. I. Frenkel and T. Kontorova, Zh. Eksp. Teor. Fiz. **8**, 1340 (1938); J. Phys. (Moscow) **1**, 137 (1939).

[5]F. Parodi and R. Vaccarone, Physica C **173**, 56 (1991).

[6]Shinkosha Co., Ltd., c/o Nikko Trading Corporation, 1731 Technology Drive, Suite 665, San Jose, CA 95110.

[7]Both dc and, when necessary, pulsed (four-probe) measurements were performed in order to eliminate heating effects.

[8]J. Aomine, E. Tanaka, S. Yamasaki, K. Tani, and A. Yonekura, J. Low Temp. Phys. **74**, 263 (1989).

[9]J. H. Miller, Jr., G. H. Gunaratne, J. Huang, and T. D. Golding, Appl. Phys. Lett. **59**, 3330 (1991).

[10]To obtain these plots we assumed that $I_0L_{ij}/\phi_0=\beta_L/(|i-j|+1)^\gamma$ ($\gamma\sim 2.5$), where the values of β_L were the estimated self-inductance parameters corresponding to Figs. 1 and 2 (13 and 32, respectively). The detailed behavior did not depend critically on the value chosen for γ.

[11]H. S. J. van der Zant *et al.* IEEE Trans. Appl. Supercond. **3**, 2658 (1993).

[12]For a discussion of a similar system, involving the dynamics of charge-density waves, see S. N. Coppersmith, Phys. Rev. A **36**, 3375 (1987).